Tech Science Press

Biological function of miRNA-145-5p in angiotensin II induced renal inflammation

Bin Li[1,2,3,#]; Yucheng Sheng[4,#]; Xiaoying Xu[4]; Shengcun Wang[3]; Hongyan Song[3]; Jingyuan Li[3]; Haonan Ji[1]; Qinghua Wang[3]; Xiaodi Zhou[1,*]; Longju Qi[2,*]

[1] Department of Pediatrics, Affiliated Hospital of Nantong University, Nantong, 226001, China

[2] Department of Science and Education, Affiliated Nantong Hospital 3 of Nantong University, Nantong, 226001, China

[3] Laboratory Animal Center, Nantong University, Nantong, 226001, China

[4] Department of Gynecology and Obstetrics and Department of Oncology, Hai'an Hospital Affiliated to Nantong University, Nantong, 226600, China

Abstract: Objective: Chronic kidney disease (CKD) is a progressive disorder characterized by intricate structural and functional alterations in the kidneys, attributable to diverse causative factors. Notably, the therapeutic promise of miR-145-5p in addressing renal pathologies has been discerned. This investigation seeks to elucidate the functional role of miR-145-5p in injured kidneys by subjecting human glomerular mesangial cells (HGMCs) to stimulation with Angiotensin II (AngII). **Materials and Methods:** Cellular viability and the levels of inflammatory mediators were evaluated utilizing Cell Counting Kit-8 (CCK-8), quantitative real-time polymerase chain reaction (qRT-PCR), and western blot methodologies, both in the presence of AngII incubation and in scenarios of miR-145p overexpression and downregulation. Furthermore, the cell cycle dynamics were elucidated through Fluorescence-activated Cell Sorting (FACS) analysis. **Results:** AngII incubation induced an upregulation of miR-145-5p and inflammatory factors including Intercellular Adhesion Molecule 1 (ICAM-1), Interleukin 6 (IL-6), Interleukin 8 (IL-8), and Interleukin 1β (IL-1β). Additionally, it elevated the expression of Cyclin A2, Cyclin D1, and the G2/M cell cycle ratio. Conversely, inhibition of miR-145-5p heightened the levels of inflammatory factors and cell cycle regulators induced by AngII incubation. Reduced expression of miR-145-5p correlated with a downregulation of Interleukin 10 (IL-10) expression, concurrently promoting HGMC proliferation under AngII stimulation. Moreover, ectopic miR-145-5p expression demonstrated a reduction in inflammatory factors, cell cyclin regulators, G2/M cell cycle ratio, and overall proliferation. **Conclusion:** MiR-145-5p exhibited inhibitory effects on the inflammatory response and proliferation induced by Angiotensin II in HGMCs, showcasing its potential as a therapeutic avenue for the treatment of kidney injury.

Introduction

Chronic kidney disease (CKD) is a progressive condition marked by structural and functional transformations in the kidneys. Its prevalence among adults is substantial, posing significant morbidity and mortality risks, particularly in those with diabetes mellitus and hypertension [1]. Despite its prevalence, effective treatments for CKD are currently lacking. Diagnosis relies predominantly on diminished renal function, as evidenced by an estimated glomerular filtration rate (eGFR) less than 60 mL/min per 1.73 m², elevated

levels of renal injury markers such as albuminuria and haematuria, or imaging-detected renal pathologic changes [2]. The global burden of CKD is escalating, affecting approximately 10 percent of the adult population and resulting in around 1.2 million deaths annually. It is projected that by 2040, CKD will become the fifth leading cause of death worldwide. Projections indicate that by 2040, CKD will ascend to the fifth leading cause of death globally. The heightened prevalence, associated disability, and healthcare burden are anticipated to exert substantial pressure on individuals, families, and society at large [2].

Glomerular mesangial cell (GMC) dysfunction has received increasing attention in relation to chronic kidney disease (CKD). GMCs are the most active intrinsic cells in the glomerulus and quickly proliferate in response to stimuli such as immune complexes, macromolecules, hypoxia, and high glucose environments, driving pathological changes [3].

Activated and hyperplastic GMCs induce oxidative stress and produce vasoactive substances and cytokines, damaging themselves through autocrine signaling and affecting other cells through paracrine signaling [4]. This process accelerates the progression of various glomerular diseases. Anti-angiotensin II receptor type-1 (AT1R) and Anti-angiotensin II receptor type-2 (AT2R) receptors are found in GMCs [5]. GMCs also possess an important endogenous antioxidant system that scavenges free radicals [6]. Reactive oxygen species play a role in the regulation of angiotensin II receptor-mediated glomerular cell proliferation and immune responses [7]. Therefore, further research is needed to investigate the relationship between the inflammatory response and cell injury in GMCs. Angiotensin II (AngII) is highly concentrated in the kidney and plays a crucial role in kidney pathology. AngII is an octapeptide that is hydrolyzed from angiotensin by angiotensin-converting enzyme [8]. It is one of the primary bioactive components of the renin-angiotensin system (RAS) and has a significant impact on cell growth, proliferation, migration, apoptosis, and inflammatory response [9,10]. By binding to angiotensin receptors, AngII initiates various physiological processes that promote arteriolar contraction, thereby increasing blood pressure through stimulation of the vascular smooth muscle [11]. Studies have shown that AngII promotes the release of Monocyte Chemotactic Protein 1 (MCP-1) from GMCs, which consequently enhances the proliferation of parietal epithelial cells (PECs) to form crescent bodies [12]. Overexpression of Ang II activates multiple intracellular signal transduction systems through interactions with various cytokines and growth factors, promoting GMC proliferation, hypertrophy, and involvement in vascular remodeling [13].

MicroRNAs (miRNAs), approximately 22-nucleotide-long endogenous single-stranded non-coding RNA molecules, play a pivotal role in cellular processes, including differentiation, metabolism, aging, autophagy, and apoptosis, by orchestrating mRNA degradation or translational inhibition through recruitment of the RNA-induced silencing complex (RISC) [14,15]. The dysregulation of miRNA expression has been a focal point in recent studies investigating renal diseases [16]. Studies employing selective Dicer deletion in mouse podocytes unveiled clinically relevant abnormalities such as proteinuria, kidney failure, and mortality, characterized by glomerulosclerosis, foot process effacement, uneven glomerular basement membrane, podocyte death, mesangial enlargement, capillary dilation, and podocyte depletion [17]. Transcriptome sequencing highlighted substantial expression of miR-192, miR-194, miR-204, miR-215, and miR-216 in the kidney [18,19]. In glomeruli, elevated miR-145-5p acted protectively against immunological injury in glomerulonephritis [19]. In rats with chronic glomerulonephritis (CGN), featuring mesangial cell proliferation and inflammatory responses, abnormal upregulation of miR-145-5p was observed. Both *in vivo* and *in vitro* tests demonstrated that miR-145-5p mitigates rat mesangial cell proliferation and inflammatory responses by modulating the Protein kinase B (Akt)/Glycogen synthase kinase (GSK) pathway via Chemokine (C-X-C motif) ligand 16 (CXCL16) targeting [20]. Furthermore, miR-145 regulates the progression of Lupus nephritis through the Colony-stimulating factor 1 (CSF1)-mediated Janus kinase (JAK)/ Signal transducer and activator of transcription (STAT) pathway [21]. Dioscin alleviated hepatorenal damage induced by methotrexate through modulation of miR-145-5p-mediated oxidative stress [22].

Chronic Kidney Disease (CKD), a prevalent nephropathy, induces kidney injury with significant implications for patients' quality of life. Despite its impact, the role of miRNAs and their associated mechanisms in CKD has received insufficient attention. In this study, we employed human glomerular mesangial cells (HGMCs) and induced renal injury by exposing them to angiotensin II. Through the manipulation of miR-145-5p expression via ectopic transfection or knockdown techniques, we investigated its regulatory role in immune response, cell cycle, and proliferation. Our findings suggest that miR-145-5p holds potential as a novel biological marker for the diagnosis and treatment of glomerulonephritis.

Materials and Methods

Cell culture and transfection

Human glomerular mesangial cells (HGMCs) were obtained from ScienCell Research Laboratories (Carlsbad, CA, USA, #4200), and cultured in Dulbecco's Modified Eagle Medium (DMEM) (Gibco, Carlsbad, California, USA, 10-092-CRVC) containing 10% of Fetal bovine serum (FBS) (Gibco, Carlsbad, California, USA, 10099141C) and 100 U/ml penicillin-streptomycin (Gibco, Carlsbad, California, USA, 15140122) under 37°C in a 5% CO_2 incubator. AngII stimulation group (final concentration of AngII was 100 nM), control group, miR-145-5p mimic transfection group and miR-145-5p inhibitor group were established on 6-well plates 6 h after cell inoculation, cells were collected at different time points based on the requirements of each experiment. All the scramble (5′-UCACAACCUCCUA GAAAGAGUAGA-3′), mimic (5′-GUCCAGUUUUCCCA GGAAUCCCU-3′) and inhibitor (5′-AGGGA UUCCUGGGAAAACUGGAC-3′) were synthesized by Ribobio Company (Guangzhou, China). Before transfection, the frozen mimic and inhibitor were taken out and thawed on an ice box. 2.5 μL mimic or 5.0 μL inhibitor was added in 250 μL opti-MEM solution (Yobibio, Shanghai, China, U21-08100A) in tube A to make the final working concentration to 50 nM. 5 μL Lipofectamine 2000 (Invitrogen, Carlsbad, California, USA, 11668019) was added to 250 μL opti-MEM solution in tube B. Solution in tube B was added to tube A and gently mixed. The mixture was sat still for 20 min at room temperature. New fresh complete medium was supplied to the transfection system. Cell samples were collected at a given time for subsequent laboratory analysis. Current study was approved by the Ethics Committee of Nantong University (Nantong, China; approval no. S20160305-601).

TABLE 1

Primer sequence of target genes (*Homo sapiens*)

Gene name	Forward Sequence (5′ to 3′)	Reverse Sequence (5′ to 3′)
GAPDH	GGAGCGAGACCCCACTAAC	GGCGGAGATGATGACCCT
IL-1β	GAAGAAGAGCCCATCCTCTG	TCATCTCGGAGCCTGTAGTG
IL-6	GTCAACTCCATCTGCCCTTC	TGTGGGTGGTATCCTCTGTG
IL-2	CAGCGTGTGTTGGATTTGAC	TGATGCTTTGACAGATGGCTA
IL-10	CGACGCTGTCATCGATTTCTC	CAGTAGATGCCGGGTGGTTC
ICAM-1	TGTCCCCCTCAAAAGTCATC	TTGCTCAGTTCATACACCTTCC
IL-8	TCTGGACCCCAAGGAAAAC	GCATCTGGCAACCCTACAAC
CyclinA2	GTTTAGCAATGTTTTTGGGAGA	TTGAGGTAGGTCTGGTGAAGG
CyclinD1	AACAGAAGTGCGAGGAGGAG	GATGGAGTTGTCGGTGTAGATG
miR-145-5p	TCGGCAGGGTCCAGTTTTCCCA	CTCAACTGGTGTCGTGGA
U6 snRNA	GGAGCGAGATCCCTCCAAAAT	GGCTGTTGTCATACTTCTCATGG

Quantitative real-time polymerase chain reaction (qRT-PCR) and RNA

The collected cell samples were thawed and utilizing Trizol buffer produced by Vazyme company (Vazyme, Nanjing, China, R401-01), the total RNA was isolated according to the protocol from supplier. RNA sediments were resolved and thermo Fisher Scientific's NanoDrop 2000 was used to calculate concentration. RNA strands were reversely transcribed into cDNA with synthesis kit (Vazyme, Nanjing, China, R212) and quantified by SYBR Green Mix (Vazyme, Nanjing, China, Q141) under the reaction condition as below: 95℃ 5 min; 95℃ 10 s, 60℃ 30 s, 40 cycles. Additionally, cDNA synthesis for miRNA detection was generated by miRNA synthesis kit (Vazyme, Nanjing, China, MR101) and checked by miRNA Universal SYBR Mix (Vazyme, Nanjing, China, MQ101) under the reaction condition as below: 95℃ 5 min; 95℃ 10 s, 60℃ 30 s, 40 cycles. Samples were examined in triplicate and $2^{-\Delta\Delta Ct}$ method was used to standardize Ct values to the expression of the housekeeping genes GAPDH or U6 snRNA. Primers were selected by Primer 3 online tools and blasted for its uniqueness. The primer sequences were detailed in Table 1.

Western blot assay

Cell lysis was performed using radio-immunoprecipitation assay buffer (RIPA, P0013B, Beyotime, Nantong, China) and total protein was extracted through centrifugation and followed by quantification using the BCA protein assay kit (E111, Vazyme, Nanjing, China). Equivalent protein amounts were loaded into 8%~15% sodium dodecyl sulfate-polyacrylamide gel electrophoresis at 20 mA per gel, and subsequently transferred from gels to polyvinylidene difluoride membranes. After blocking with 5% defatted milk for 1 h at room temperature (RT). Membranes were incubated with primary antibodies of IL-6 (1:1000, ab9324, Abcam), Cyclin A2 (1:1000, ab181591, Abcam), ICAM-1 (1:1000, ab109361, Abcam), IL-10 (1:1000, ab133575, Abcam), β-actin (1:5000, ab179467, Abcam) at 4℃ for one night. HRP-conjugated secondary antibodies (1:10000,

ab205718 and ab205719, Abcam) were applied to the washed membranes for 2 h at room temperature. Blots were revealed by ECL solution (E412, Vazyme, Nanjing, China). All bands were exposed with a Tanon 5200 system and interpreted by ImageJ software, and β-actin was taken as internal control.

CCK-8 assay

A cell suspension was prepared and seeded in 96-well plates with 2000 cells/well. Subsequently, 10 μL of Cell Counting Kit 8 (CCK8) solution (A311, Vazyme, Nanjing, China) was introduced into each well at intervals of 0, 12, 24, 48, and 72 h. The CCK8 solution should be added along the wall of the plate and shake gently to avoid air bubbles. And the plates were incubated for extra 2 h at 37℃. The optical density was detected under 450 nm with a microplate reader (Multiskan FC, Thermo Fisher Scientific, Carlsbad, CA, USA). All results were gathered and computed using the formula below. Viability rate = 100 × (OD amount of experimental group/OD amount of control group).

Enzyme-linked immunosorbent assay kit

The levels of supernatant IL-1β and IL-8 were determined by human IL-1β Elisa kit (DLB50, R&D System, Minneapolis, MN) and IL-8 Elisa kit (D8000C, R&D System, Minneapolis, MN), respectively, following the manufacturer's indications.

Flow cytometry

For cell cycle analysis, cells underwent two washes with pre-cooled PBS and were then dislodged using Trypsin without EDTA (Gibco, Carlsbad, California, USA, 15050065). The trypsin was deactivated by complete culture medium containing 5% FBS. Subsequently, cells were harvested by centrifugation with 1000 rpm for 5 min at RT. The collected cells were fixed with precooled 100% ethanol solution for 20 min at 4℃, and then stained in propidium iodide (PI) at 37℃ for 30 min. Cell cycles were analyzed on a FACScalibur flow cytometer (BD, Franklin Lakes, NJ, USA), and estimated using CellQuest software (BD, Franklin Lakes, NJ, USA).
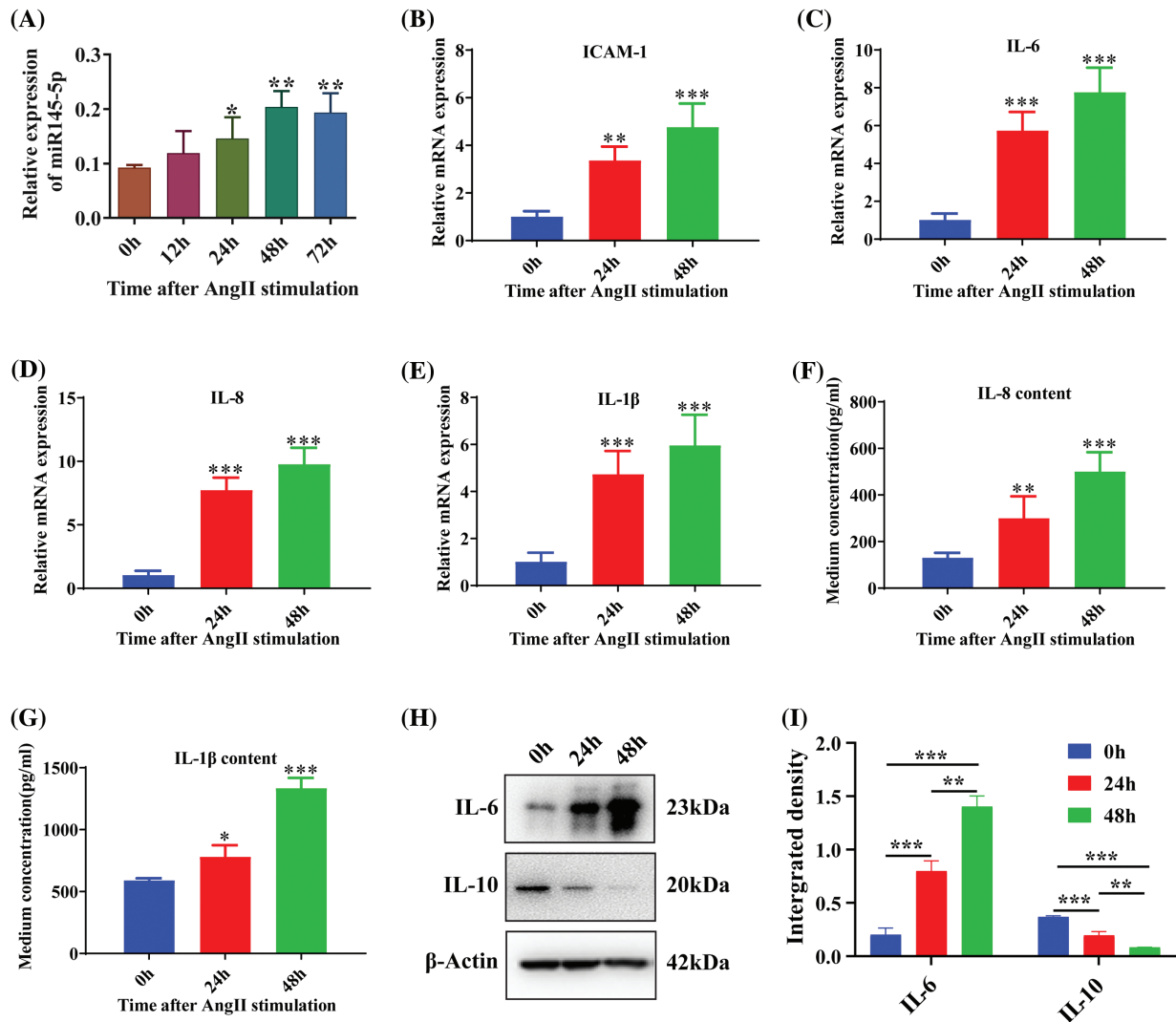
FIGURE 1. AngII boosted the inflammation response in HGMCs. (A) Expression levels of miR-145-5p at 0, 12, 24, 48 and 72 h after AngII incubation. (B–E) Transcriptional expression of ICAM-1, IL-6, IL-8 and IL-1β detected by qRT-PCR. (F and G) Content of IL-8 and IL-1β in supernatant checked by Elisa kits. (H) Protein expression of IL-6 detected by western blot. (I) Relative grey density-based statistical analysis of the western blot data. AngII had a final concentration of 100 nM. All samples for PCR and western blot were harvested at 24 and 48 h post AngII treatment. N = 8 for mRNA detection, N = 5 for Elisa investigation, and N = 3 for western blot analysis. *$p < 0.05$, **$p < 0.01$, ***$p < 0.001$.

Statistical evaluation

SPSS Statistics software (version 24.0) was taken into the statistical evaluation. All testimonies were given as mean ± standard deviation ($\bar{X}$±SD) and significance was assessed by Student's *t*-test between two groups, while 1-way analysis of variance (ANOVA) with Tukey's multiple comparisons test was used to evaluate comparisons among multi-groups. A 2-tailed test was utilized for *p* value calculation, and significance was established for *p* values less than 0.05.

Results

AngII boosted the inflammation response in HGMCs

The expression of miR-145-5p showed a significant upregulation at 24 h ($p < 0.05$), 48 h ($p < 0.01$), and 72 h ($p < 0.01$) post-incubation with 100 nM AngII (Fig. 1A). Furthermore, the mRNA levels of inflammatory factors, including ICAM-1 (24 h, $p < 0.01$; 48 h, $p < 0.001$), IL-6 (24 h, $p < 0.001$; 48 h, $p < 0.001$), IL-8 (24 h, $p < 0.001$; 48 h,

$p < 0.001$), and IL-1β (24 h, $p < 0.01$; 48 h, $p < 0.001$), were evaluated at 24 and 48 h after AngII treatment (Figs. 1B–1E). Additionally, the concentration of IL-8 and IL-1β in the culture medium was measured using Elisa, revealing an increase after AngII treatment (Figs. 1F and 1G). Subsequent western blot analysis indicated a noticeable increase in IL-6 protein expression at 24 h ($p < 0.001$) and 48 h ($p < 0.001$), along with a reduction in IL-10 protein expression at 24 h ($p < 0.001$) and 48 h ($p < 0.001$) compared to the control group (Figs. 1H and 1I). Collectively, these findings suggest that AngII significantly elevates miR-145-5p expression and induces a distinct upregulation in typical inflammatory factors.

AngII reshaped the cell cycle in HGMCs

To investigate the impact of Angiotensin II (Ang II) on the cell cycle, we examined the mRNA expression levels of Cyclin A2 and Cyclin D1. The results revealed a significant increase in both Cyclin A2 ($p < 0.001$; Fig. 2A) and Cyclin D1 ($p < 0.001$; Fig. 2B) after 24 h. Furthermore, the protein
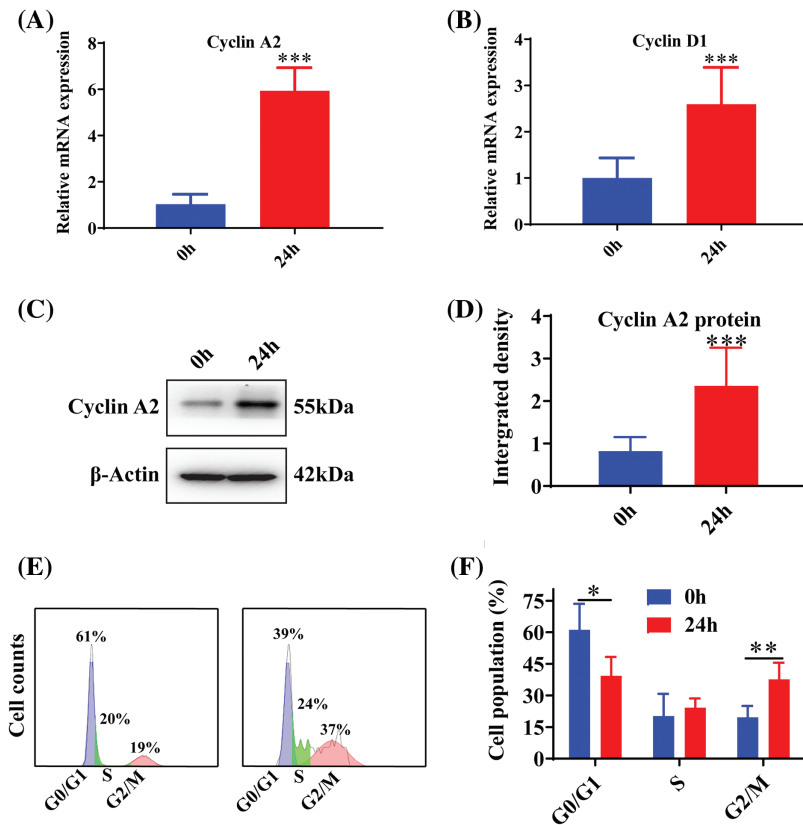
FIGURE 2. AngII reshaped the cell cycle in HGMCs. (A and B) Transcriptional expression of Cyclin A2, and Cyclin D1 was quantified by qRT-PCR. (C) Protein expression of Cyclin A2 was revealed by western blot. (D) Western blot data statistically analyzed based on relative grey density. (E) Cell cycle variations of HGMCs that stimulated with AngII for 24 h were investigated by FACs analysis. (F) Statistical analysis of the FACs results to reveal the distribution of different phases in cell cycle. The final concentration of AngII was 100 nM. All samples for PCR, western blot and FACs were collected at 24 h after AngII incubation, N = 8 for mRNA inspection, and N = 3 for western blot investigation and FACs examination. $*p < 0.05$, $**p < 0.01$, $***p < 0.001$.

expression of Cyclin A2 also showed a significant enhancement at 24 h following Ang II challenge ($p < 0.001$; Figs. 2C and 2D). To further assess the alterations in the cell cycle of HGMCs, flow cytometry was employed. The findings indicated that incubation with Ang II led to a reduction in the fraction of cells in the G0/G1 stage, accompanied by an increase in the proportion of cells in the G2/M stage ($p < 0.01$; Figs. 2E and 2F). These observations suggest that Ang II can modulate cell cycle distribution by upregulating the expression levels of genes associated with the cell cycle.

Downregulation of miR-145-5p accelerated the inflammatory reaction in HGMCs
The microRNA inhibitor demonstrated a significant knockdown efficiency at both 24 h ($p < 0.05$) and 48 h ($p < 0.001$) post-transfection (Fig. 3A). The treatment of AngII resulted in a reduction in the expression of IL-10 ($p < 0.001$), and the inhibition of miR-145-5p notably decreased IL-10 expression compared to control cells ($p < 0.001$, Fig. 3B). Additionally, AngII noticeably increased the expression of ICAM-1 ($p < 0.001$, Fig. 3C), IL-6 ($p < 0.001$, Fig. 3D), and IL-1β ($p < 0.001$, Fig. 3E), while the application of the miRNA-145-5p inhibitor further enhanced the expression of ICAM-1 ($p < 0.001$, Fig. 3C), IL-6 ($p < 0.001$, Fig. 3D), and IL-1β ($p < 0.001$, Fig. 3E). Moreover, the protein levels of ICAM-1 ($p < 0.001$) and IL-6 ($p < 0.01$) increased after AngII incubation, and were further boosted by the transfection of the miR-145-5p inhibitor (ICAM-1, $p < 0.05$; IL-6, $p < 0.05$, Figs. 3F and 3G). In contrast, the inhibitor significantly downregulated the protein expression of IL-10 compared with the control

cells ($p < 0.001$, Figs. 3F and 3G). Overall, the inhibition of miR-145-5p expression hindered the expression levels of anti-inflammatory factors, concurrently augmenting the expression of pro-inflammatory factors.

Inhibition of miR-145-5p variated HGMCs cell cycle
To explore the impact of inhibiting miR-145-5p on the cell cycles of HGMCs under the influence of Angiotensin II (AngII), we scrutinized the transcriptional alterations of Cyclin A2 and Cyclin D1. The results revealed that the adoption of the inhibitor enhanced the expression of Cyclin A2 ($p < 0.05$, Fig. 4A) and Cyclin D1 ($p < 0.05$, Fig. 4B) compared to cells treated with AngII. Flow cytometry results showed that inhibiting miR-145-5p decreased the cell population in the G0/G1 phase ($p < 0.05$, Figs. 4C and 4D), while increasing the fraction of cells in the G2/M phase ($p < 0.01$, Figs. 4C and 4D). Furthermore, cell viability increased after incubation with AngII for 24 h ($p < 0.001$), 48 h ($p < 0.001$), and 72 h ($p < 0.001$) compared to control cells, and the inhibition of miR-145-5p enhanced cell viability compared to AngII-treated cells at 24 h ($p < 0.001$), 48 h ($p < 0.001$), and 72 h ($p < 0.001$, Fig. 4E). Additionally, the treatment with the miR-145-5p inhibitor increased Cyclin A2 protein levels compared to cells incubated with AngII ($p < 0.01$, Figs. 4F and 4G). In conclusion, inhibiting miR-145-5p promoted cell cycle regulators and increased the proportion of cells in the G2/M phase.

Upregulation of miR-145-5p ameliorated the inflammation in HGMCs
The ectopic expression of miR-145-5p demonstrated a significant increase at 24 h ($p < 0.01$), 48 h ($p < 0.001$), and
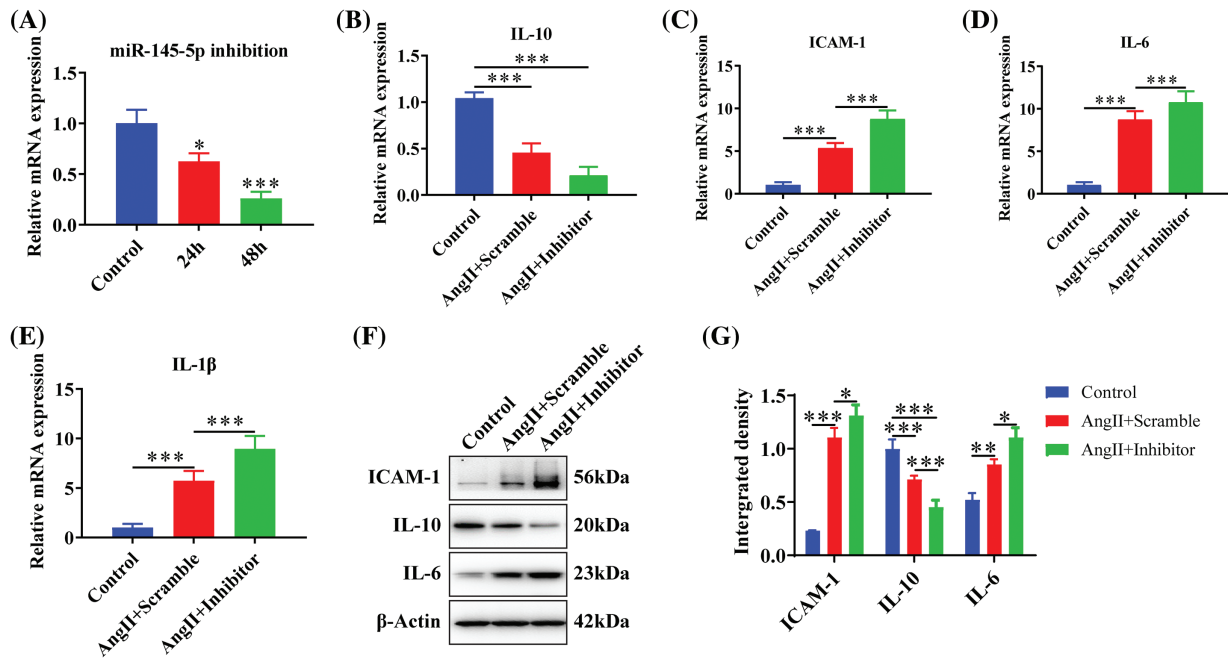
FIGURE 3. Downregulation of miR-145-5p accelerated the inflammation in HGMCs. (A) Knockdown efficiency of miR-145-5p was confirmed by qRT-PCR. (B–E) Transcriptional expression of IL-10, ICAM-1, IL-6, and IL-1β detected by qRT-PCR. (F) ICAM-1, IL-6, and IL-10 protein expression was checked by western blot. (G) Relative grey density-based statistical analysis of the western blot data. AngII had a final concentration of 100 nM. All samples for PCR and western blot were collected at 24 h after AngII incubation, N = 8 for mRNA detection, N = 5 for Elisa survey, and N = 3 for western blot analysis. *$p < 0.05$, **$p < 0.01$, ***$p < 0.001$.

72 h ($p < 0.01$) post-transfection (Fig. 5A). Furthermore, overexpression of miR-145-5p significantly decreased the expression levels of ICAM-1 ($p < 0.001$, Fig. 5B), IL-6 ($p < 0.001$, Fig. 5C), and IL-1β ($p < 0.001$, Fig. 5D), while significantly increasing the expression of IL-10 ($p < 0.001$, Fig. 5E) compared to AngII-stimulated cells. Furthermore, the protein levels of IL-10 were significantly increased in the presence of miR-145-5p overexpression compared to AngII-treated cells ($p < 0.001$, Figs. 5F and 5G) or control cells ($p < 0.001$, Figs. 5F and 5G). Conversely, ectopically expressed miR-145-5p mimic decreased the protein expression of ICAM-1 ($p < 0.001$, Figs. 5F and 5G) and IL-6 ($p < 0.01$, Figs. 5F and 5G). In summary, miR-145-5p exhibited an inhibitory effect on the AngII-induced inflammatory reaction.

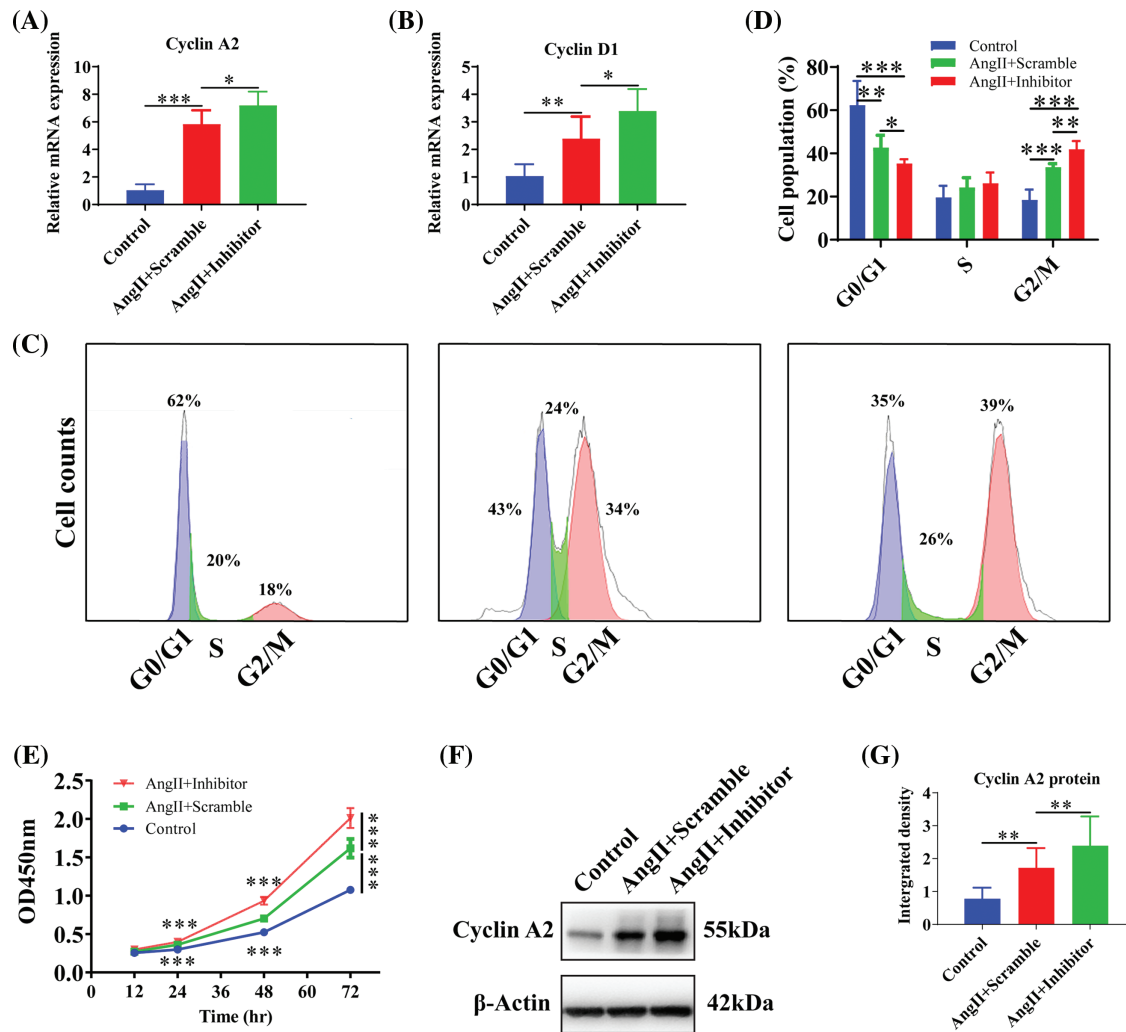*Raised miR-145-5p inhibited HGMCs cell cycle*

To explore the effects of AngII and miR-145-5p mimic treatment on the cell cycle of HGMCs, we examined the transcriptional expression of cell cycle regulators. The results demonstrated a significant downregulation in the expression of Cyclin A2 ($p < 0.001$, Fig. 6A) and Cyclin D1 ($p < 0.001$, Fig. 6B) in cells treated with AngII. Furthermore, the overexpression of miR-145-5p mimic hindered the protein expression of Cyclin A2 compared to the cells incubated with AngII ($p < 0.001$, Figs. 6C and 6D). Flow cytometry analysis revealed that the fraction of G0/G1 cells increased in cells transfected with the mimic ($p < 0.05$, Figs. 6E and 6F), while the proportion of G2/M cells decreased in cells overexpressing the mimic compared to AngII-treated cells ($p < 0.05$, Figs. 6E and 6F). Additionally, the cell viability was significantly decreased in HGMCs with miR-145-5p overexpression at 24 h ($p < 0.001$), 48 h ($p < 0.001$),

and 72 h ($p < 0.001$, Fig. 6G). In conclusion, the ectopically overexpressed miR-145-5p resulted in a decrease in the cell cycle progression of HGMCs.

Discussion

The present study unearthed miR-145-5p as a protective non-coding RNA against kidney injury. The results demonstrated the following findings: (1) AngII increased the inflammatory response, the expression of miR-145-5p, and the ratio of G2/M cell cycle in HGMCs; (2) upregulation of miR-145-5p reduced the inflammatory reaction, cell proliferation, and the ratio of G2/M cell cycle; (3) downregulation of miR-145-5p elevated the inflammation levels, cell proliferation, and the ratio of G2/M cell cycle.

Glomerular mesangial cells (GMCs) perform various functions such as contraction, phagocytosis, and production of extracellular matrix, which play a crucial role in maintaining normal kidney function and the development of renal lesions [23]. Mature GMCs *in vivo* exhibit a quiescent phenotype under physiological conditions, characterized by slow proliferation and a dynamic balance between secretion and degradation of extracellular matrix. However, under pathological conditions, such as inflammation and injury, GMCs can become activated and acquire a proliferative or secretory phenotype, characterized by hyperproliferation and secretion of extracellular matrix [24,25]. Activation of GMCs is a common response to various harmful stimuli in the glomerulus. *In vivo* and *ex vivo* studies have shown that various injurious factors and harmful substances can activate GMCs and promote their proliferation. GMCs were the most active intrinsic cells within the glomerulus in patients with CKD. Under

FIGURE 4. Inhibition of miR-145-5p variated HGMCs cell cycles. (A and B) The transcriptional expression levels of Cyclin A2, and Cyclin D1 was quantified by qRT-PCR under conditions of miR-145-5p inhibition. (C) Cell cycle variations of HGMCs after miR-145-5p inhibition under treatment of AngII were investigated by FACs analysis. (D) Statistical analysis of the FACs results to reveal the distribution of different phases in cell cycle. (E) Detection of the cell survival rate after inhibition of miR-145-5p under the treatment with AngII using the CCK-8 assay. (F) Protein expression of Cyclin A2 was analyzed by western blot. (G) Relative grey density based statistical analysis of western blot results. The final concentration of AngII was 100 nM. All samples for PCR, western blot and FACs were collected at 24 h after AngII incubation, N = 8 for mRNA detection and cell survival rate examination; and N = 3 for western blot analysis and FACs analysis. $*p < 0.05$, $**p < 0.01$, $***p < 0.001$.

glomerular conditions, they become activated and transition into a secretory and proliferative state [3,26]. Activated GMCs proliferated rapidly and secreted numerous inflammatory mediators and This, in turn, led to hyperplasia of the cell matrix and infiltration of numerous immune cells resulting in glomerular fibrosis [27,28]. Studies have confirmed that AngII stimulation induces proliferation and secretion of inflammatory mediators, which is one of the potential pathogenic mechanisms of chronic kidney disease [29,30]. However, the molecular mechanisms underlying how AngII promotes GMC proliferation and secretion of inflammatory mediators are still unknown.

Angiotensin II were derived from angiotensin I by hydrolyzing of angiotensin converting enzyme and specifically combined with a variety of angiotensin receptors [31]. It was a key regulator in renin-angiotensin system and report showed that AngII stimulated mesangial cells

secreted MCP-1 that promoted the excessive proliferation of parietal epithelial cells by paracrine regulation. Similarly, in this study, AngII promotes the release of inflammatory factors from HGMCs and enhances their proliferation.

Since the discovery of small non-coding RNAs, microRNAs (miRNAs) have garnered significant attention from researchers. These miRNAs serve as critical components of the RNA-induced silencing complex (RISC) and play essential roles in regulating various aspects of RNA transcription. This includes their involvement in the regulation of targeted mRNA transcription, splicing, translation, and chromatin modification [32]. Notably, a study identified six miRNAs, namely mmu-miR-192, rno-miR-192, rno-miR-194, rno-miR-203, rno-miR-450, and rno-miR-34a, as preferentially expressed in the renal cortex, while the renal medulla contained eleven rat miRNAs, including let-7e, miR-30c, miR-24, miR-27a, miR-23a, miR-27b, miR-200b, miR-99a, miR-125a, miR-200c, and miR-
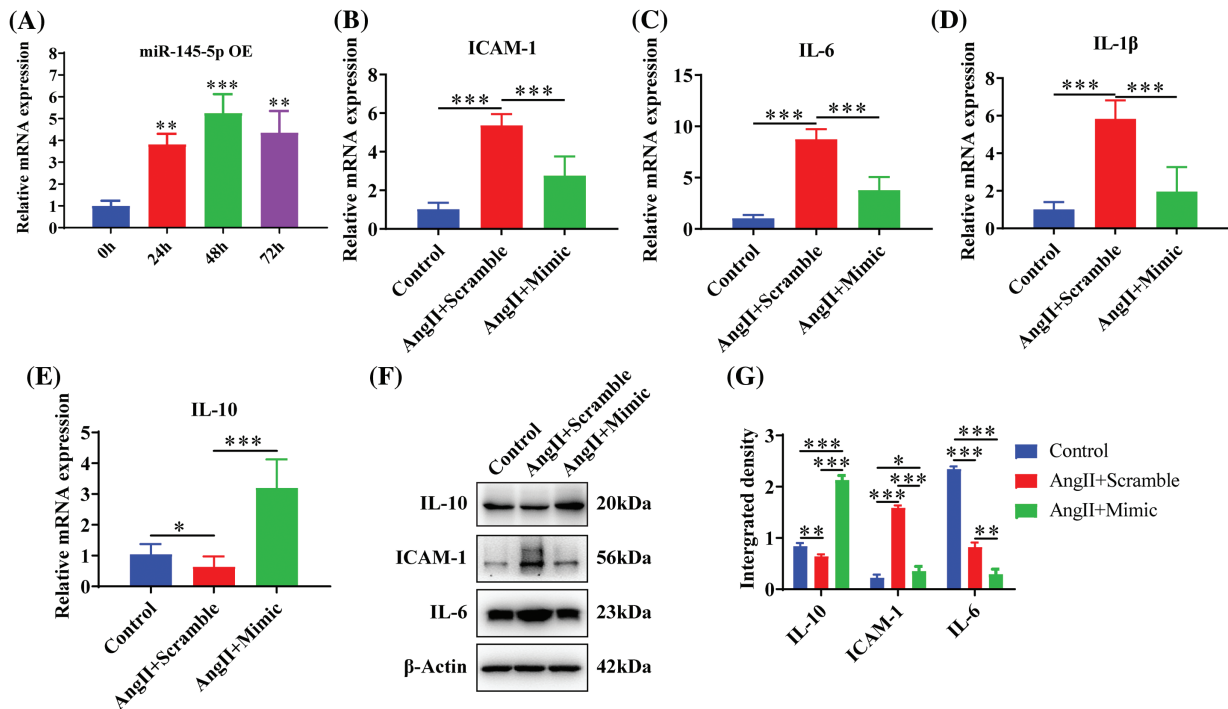
FIGURE 5. Upregulation of miR-145-5p ameliorated the inflammation in HGMCs. (A) Overexpression efficiency of miR-145-5p was confirmed by qRT-PCR. (B–E) Transcriptional expression of ICAM-1, IL-6, IL-1β and IL-10 was detected by qRT-PCR after miR-145-5p overexpression. (F) Protein expression of IL-10, ICAM-1, and IL-6 was analysed by western blot. (G) Statistical analysis of the western blot results on the ground of relative grey density. The final concentration of AngII was 100 nM. All samples for PCR and western blot were collected at 24 h after AngII incubation, N = 8 for mRNA detection, N = 5 for Elisa investigation, and N = 3 for western blot analysis. $^{*}p < 0.05$, $^{**}p < 0.01$, $^{***}p < 0.001$.

125b. Furthermore, miR-126 was found to be located in glomerular endothelial cells, miR-145 was predominantly distributed in mesangial cells, and miR-30a was found to be highly expressed in podocytes [33]. The miR-205 and miR-200 families, which comprise miR-200a, miR-200b, miR-200c, miR-141, and miR-429, have been reported to participate in the transition of epithelial cells into mesangial cells [18]. Moreover, it was observed that miR-145-5p was highly expressed in glomeruli and protected the kidney from immune damage in cases of glomerulonephritis. Interestingly, the overexpressed miR-145-5p was demonstrated to hinder proliferation and inflammatory responses in human glomerular mesangial cells (HGMCs), suggesting its crucial role in regulating mesangial cell reactions during hazardous conditions. Conversely, the hindrance of miR-145-5p resulted in increased inflammation and proliferation in HGMCs. Unfortunately, there are currently no reports regarding the direct or indirect interplaying of miR-145-5p and IL-10. However, based on the observations made in this study, it is possible to speculate a connection between the two. To explore this further, we examined potential regulatory downstream genes of miR-145-5p in the database and identified XBP1 and XBP2 as potential transcriptional regulators of IL-10. Thus, miR-145-5p may affect the expression of IL-10 by modulating the expression of either or both of these genes, ultimately affecting local immune responses. In conclusion, miR-145-5p plays a vital role in combating the detrimental effects induced by AngII.

Cell proliferation relies on the arrangement of the cell cycle, which is monitored by cell cycle checkpoints involving cyclins and cyclin-dependent kinases (CDKs). Cyclins are key regulators of the G1/S and G2/M phase transitions. While Cyclin A2 is widely distributed, Cyclin A1 is primarily localized in the testis. Cyclin A2 regulates the transitions between the G1/S, S, and G2/M phases of the cell cycle. It accomplishes this by activating Cdk1, Cdk2 and maintaining escalated levels from the S phase till early mitosis [34]. Mice with a mutation preventing Cyclin A2 expression exhibit chromosomal instability and prone to tumors. Therefore, Cyclin A2 is frequently expressed at high levels in human malignancies due to its association with cell proliferation. Furthermore, Cyclin A2 has been demonstrated to participate in regulating cytoskeleton dynamics and cell motility [35]. Type D cyclins, in conjunction with their own catalytic allies CDK4 and CDK6, play an important role in regulating restriction points during the G1 phase and achieving the conversion from G1 to S phase [36]. Cyclin D proteins keep cells in a quiescent state when growth signals are absent, but upregulation of Cyclin D1 leads to uncontrolled cell proliferation, as documented in breast cancer, lung cancer, colon cancer, oral cancers, and melanoma [37–40]. Former studies have illustrated that miR-145-5p can modulate cell cycle progression by regulating various targets, including ETS proto-oncogene 2 (ETS2) [41], Sp1 transcription factor (SP1) [42], Spermatogenesis associated serine rich 2 (SPATS2) [43], Tripartite motif containing 2 (TRIM2) [44], DNA topoisomerase II alpha (TOP2A) [45], and ADP ribosylation factor 6 (ARF6) [46]. Under AngII stimulation, there was consistently increased expression of Cyclin A2 and Cyclin D1, resulting in boosted fraction containing cells in
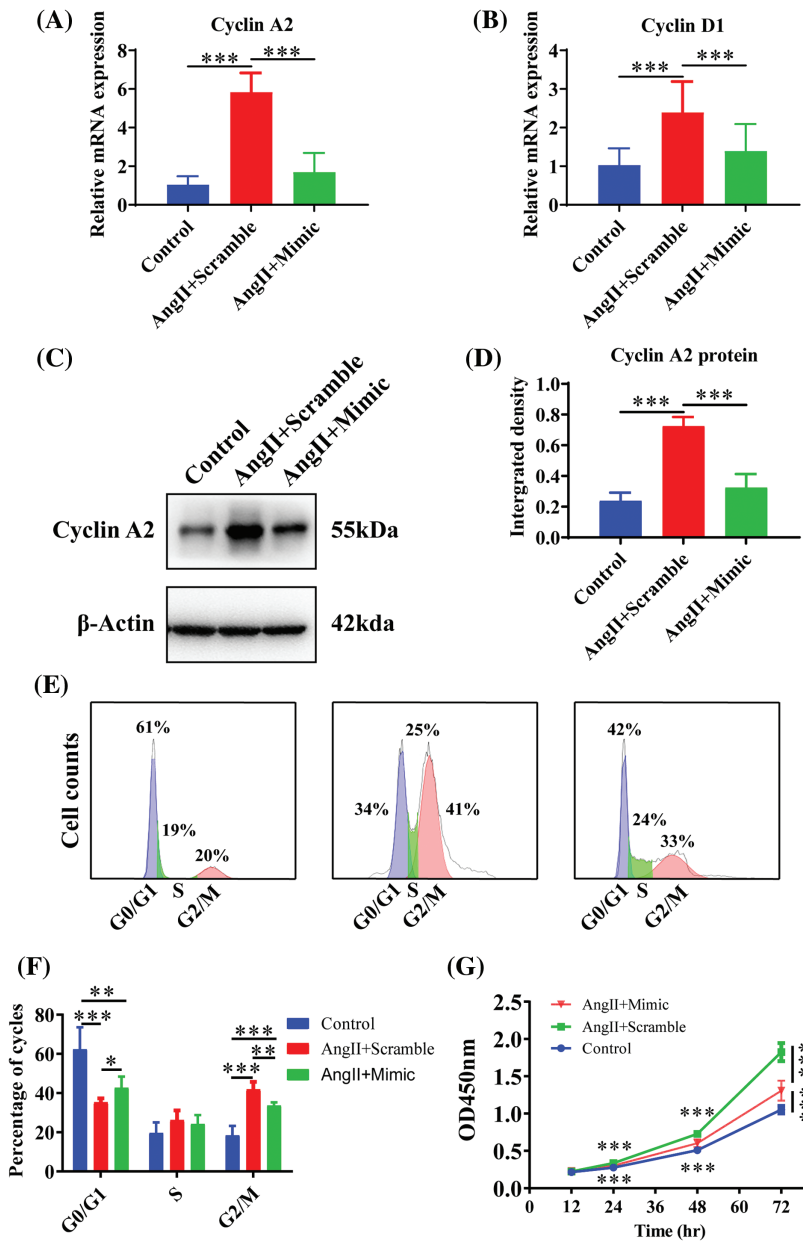
FIGURE 6. Raised miR-145-5p inhibited HGMCs cell cycle. (A and B) Under the condition of miR-145-5p overexpression, the transcriptional expression of Cyclin A2, and Cyclin D1 was quantified by qRT-PCR. (C) Protein expression of Cyclin A2 was examined by western blot. (D) The results of statistical analysis of the western blot based on relative grey density. (E) Cell cycle variations of HGMCs after miR-145-5p overexpression under treatment of AngII were investigated by FACs analysis. (F) Statistical analysis of the FACs results to reveal the distribution of different phases in cell cycle. (G) Detection of cell survival rate after overexpression of miR-145-5p under treatment of AngII by CCK-8 assay. The final concentration of AngII was 100 nM. All samples for PCR, western blot and FACs were collected at 24 h after AngII incubation, N = 8 for mRNA detection and cell survival rate examination; and N = 3 for western blot analysis and FACs analysis. $^*p < 0.05$, $^{**}p < 0.01$, $^{***}p < 0.001$.

the G2/M phase. As a result, miR-145-5p was downregulated, leading to elevated Cyclin A2 and Cyclin D1 expression, further promoting HGMC proliferation and an increased proportion of cells in the G2/M phase. Conversely, ectopic expression of miR-145-5p diminished the expression levels of Cyclin A2 and Cyclin D1, resulting in decreased cell proliferation and a higher proportion of cells in the G2/M phase. Recent research has provided additional evidence of the link between miR-145-5p and Cyclin A2 and Cyclin D1, which affect changes in the cell cycle.

This study focused on the function of miR-145-5p in coordinating the activity of mesangial cells (MCs) associated with chronic kidney disease (CKD). The outcomes illustrated that miR-145-5p had a positive impact on AngII-induced renal injury, which could potentially facilitate the testimony of novel biological targets for the diagnosis and treatment of CKD. It is important to note, however, that the findings of this study are predominantly based on experiments conducted using cell models. Therefore, further investigation utilizing animal models and patients is necessary to ascertain the specific targets regulated by miR-145-5p.

Author Contributions: BL, XZ and QJ conceived the concept, framed the experimental design, wrote the manuscript and edited the revised manuscript. YS, XX, SW, JL, HJ and QW performed the lab experiments. SW analyzed data and assembled the figures. HS and QJ confirmed the authenticity

of all the raw data. All the authors read and approved the final version of the manuscript.

Availability of Data and Materials: The data used to support the findings of this study are available from the corresponding author upon request.

Ethics Approval: The study was approved by the Ethics Committee of Nantong University (Nantong, China; approval no. S20160305-601).

Conflicts of Interest: The authors declare that they have no conflicts of interest to report regarding the present study.

References

1. Chiabotto G, Bruno S. Anti-fibrotic and anti-inflammatory effect of mesenchymal stromal cell-derived extracellular vesicles in chronic kidney disease. Biocell. 2023;47(7):1499–508.

2. Downie ML, Desjarlais A, Verdin N, Woodlock T, Collister D. Precision medicine in diabetic kidney disease: a narrative review framed by lived experience. Can J Kidney Health Dis. 2023;10:20543581231209012.

3. Sethi S, de Vriese AS, Fervenza FC. Acute glomerulonephritis. Lancet. 2022;399(10335):1646–63.

4. Neyra JA, Chawla LS. Acute kidney disease to chronic kidney disease. Crit Care Clin. 2021;37(2):453–74.

5. Simões ESAC, Lanza K, Palmeira VA, Costa LB, Flynn JT. 2020 update on the renin-angiotensin-aldosterone system in pediatric kidney disease and its interactions with coronavirus. Pediatr Nephrol. 2021;36(6):1407–26.

6. Huang G, Zhang Y, Zhang Y, Ma Y. Chronic kidney disease and NLRP3 inflammasome: pathogenesis, development and targeted therapeutic strategies. Biochem Biophys Rep. 2023;33:101417.

7. Aranda-Rivera AK, Cruz-Gregorio A, Aparicio-Trejo OE, Pedraza-Chaverri J. Mitochondrial redox signaling and oxidative stress in kidney diseases. Biomolecules. 2021;11(8): 1144.

8. Wang K, Gheblawi M, Oudit GY. Angiotensin converting enzyme 2: a double-edged sword. Circulation. 2020;142(5): 426–8.

9. Almeida LF, Tofteng SS, Madsen K, Jensen BL. Role of the renin-angiotensin system in kidney development and programming of adult blood pressure. Clin Sci. 2020;134(6):641–56.

10. Li T, Zhang Y, Zhang T, Li Y, Xue H, Cao J, et al. Schisandrin B exerts anticancer effects on human gastric cancer cells through ROS-mediated MAPK, STAT3, and NF-κB pathways. Biocell. 2023;47(1):195–204.

11. Nistala R, Wei Y, Sowers JR, Whaley-Connell A. Renin-angiotensin-aldosterone system-mediated redox effects in chronic kidney disease. Transl Res. 2009;153(3):102–13.

12. Luo R, Yang K, Wang F, Xu C, Yang T. (Pro)renin receptor decoy peptide PRO20 protects against adriamycin-induced nephropathy by targeting the intrarenal renin-angiotensin system. Am J Physiol Renal Physiol. 2020;319(5):F930–f40.

13. Xi YY, Liu B, Yang LX, Kuang CW, Guo RW. Changes in levels of angiotensin II and its receptors in a model of inverted stress-induced cardiomyopathy. Eur J Med Res. 2014;19(1):54.

14. Rani V, Sengar RS. Biogenesis and mechanisms of microRNA-mediated gene regulation. Biotechnol Bioeng. 2022;119(3): 685–92.

15. Franczyk B, Gluba-Brzózka A, Olszewski R, Parolczyk M, Rysz-Górzyńska M, Rysz J. miRNA biomarkers in renal disease. Int Urol Nephrol. 2022;54(3):575–88.

16. Gluba-Sagr A, Franczyk B, Rysz-Górzyńska M, Ławiński J, Rysz J. The role of miRNA in renal fibrosis leading to chronic kidney disease. Biomedicines. 2023;11(9):2358.

17. Shi S, Yu L, Chiu C, Sun Y, Chen J, Khitrov G, et al. Podocyte-selective deletion of dicer induces proteinuria and glomerulosclerosis. J Am Soc Nephrol. 2008;19(11):2159–69.

18. Krupa A, Jenkins R, Luo DD, Lewis A, Phillips A, Fraser D. Loss of MicroRNA-192 promotes fibrogenesis in diabetic nephropathy. J Am Soc Nephrol. 2010;21(3):438–47.

19. Harada K, Baba Y, Ishimoto T, Kosumi K, Tokunaga R, Izumi D, et al. Suppressor microRNA-145 is epigenetically regulated by promoter hypermethylation in esophageal squamous cell carcinoma. Anticancer Res. 2015;35(9):4617–24.

20. Wu J, He Y, Luo Y, Zhang L, Lin H, Liu X, et al. MiR-145-5p inhibits proliferation and inflammatory responses of RMC through regulating AKT/GSK pathway by targeting CXCL16. J Cell Physiol. 2018;233(4):3648–59.

21. Liao W, He XJ, Zhang W, Chen YL, Yang J, Xiang W, et al. MiR-145 participates in the development of lupus nephritis by targeting CSF1 to regulate the JAK/STAT signaling pathway. Cytokine. 2022;154:155877.

22. Li Y, Gao M, Yin LH, Xu LN, Qi Y, Sun P, et al. Dioscin ameliorates methotrexate-induced liver and kidney damages via adjusting miRNA-145-5p-mediated oxidative stress. Free Radic Biol Med. 2021;169:99–109.

23. Vaughan MR, Quaggin SE. How do mesangial and endothelial cells form the glomerular tuft? J Am Soc Nephrol. 2008;19(1): 24–33.

24. Kwoh C, Shannon MB, Miner JH, Shaw A. Pathogenesis of nonimmune glomerulopathies. Annu Rev Pathol. 2006;1:349–74.

25. Liang W, Zhang Z, Yang K, Hu H, Luo Q, Yang A, et al. Genetic algorithm-optimized backpropagation neural network establishes a diagnostic prediction model for diabetic nephropathy: combined machine learning and experimental validation in mice. Biocell. 2023;47(6):1253–63.

26. Wu D, Ma R, Wang X, Yang Y. Efficacy and safety of tacrolimus in the treatment of pediatric henoch-schonlein purpura nephritis. Paediatr Drugs. 2022;24:389–401

27. Zhou F, Shao Q, Jia L, Cai C. Gut microbiota variations between henoch-schonlein purpura and henoch-schonlein purpura nephritis. Gastroenterol Res Pract. 2022;2022:4003491.

28. Gao J, Zhu X, Chen H, Jiang H, Shi M, Wei L, et al. Long non-coding NONRATG001910.2 promotes the proliferation of rat mesangial cell line HBZY-1 through the miR-339-3p/CTNNB1 axis. Front Genet. 2022;13:834144.

29. Maranduca MA, Clim A, Pinzariu AC, Statescu C, Sascau RA, Tanase DM, et al. Role of arterial hypertension and angiotensin II in chronic kidney disease (Review). Exp Ther Med. 2023;25(4):153.

30. Alshahrani S. Renin-angiotensin-aldosterone pathway modulators in chronic kidney disease: a comparative review. Front Pharmacol. 2023;14:1101068.

31. Ruster C, Wolf G. The role of the renin-angiotensin-aldosterone system in obesity-related renal diseases. Semin Nephrol. 2013; 33(1):44–53.

32. Ha M, Kim VN. Regulation of microRNA biogenesis. Nat Rev Mol Cell Biol. 2014;15(8):509–24.

33. Huang TC, Pinto SM, Pandey A. Proteomics for understanding miRNA biology. Proteomics. 2013;13(3–4):558–67.

34. Kanakkanthara A, Jeganathan KB, Limzerwala JF, Baker DJ, Hamada M, Nam HJ, et al. Cyclin A2 is an RNA binding protein that controls Mre11 mRNA translation. Science. 2016;353(6307):1549–52.

35. Zaveri L, Dhawan J. Inducible expression of Oct-3/4 reveals synergy with Klf4 in targeting Cyclin A2 to enhance proliferation during early reprogramming. Biochem Biophys Res Commun. 2022;587:29–35.

36. Gonzalez-Ruiz L, Gonzalez-Moles MA, Gonzalez-Ruiz I, Ruiz-Avila I, Ayen A, Ramos-Garcia P. An update on the implications of cyclin D1 in melanomas. Pigment Cell Melanoma Res. 2020;33(6):788–805.

37. Garcia NG, Gonzalez-Moles MA, Ruiz-Avila I, Bravo M, Ramos-Garcia P, Minicucci EM, et al. Asymmetrical proliferative pattern loss linked to cyclin D1 overexpression during malignant transformation of the lip epithelium. J Eur Acad Dermatol Venereol. 2016;30(8):1315–20.

38. Ramos-Garcia P, Bravo M, Gonzalez-Ruiz L, Gonzalez-Moles MA. Significance of cytoplasmic cyclin D1 expression in oral oncogenesis. Oral Dis. 2018;24(1–2):98–102.

39. Ramos-Garcia P, Gonzalez-Moles MA, Ayen A, Gonzalez-Ruiz L, Gil-Montoya JA, Ruiz-Avila I. Predictive value of *CCND1/* cyclin D1 alterations in the malignant transformation of potentially malignant head and neck disorders: systematic review and meta-analysis. Head Neck. 2019;41(9):3395–407.

40. Marzuka-Alcala A, Gabree MJ, Tsao H. Melanoma susceptibility genes and risk assessment. Methods Mol Biol. 2014;1102:381–93.

41. Qiao L, Li RX, Hu SG, Liu Y, Liu HQ, Wu HJ. microRNA-145-5p attenuates acute lung injury via targeting ETS2. Kaohsiung J Med Sci. 2022;38(6):565–73.

42. Mei LL, Wang WJ, Qiu YT, Xie XF, Bai J, Shi ZZ. miR-145-5p suppresses tumor cell migration, invasion and epithelial to mesenchymal transition by regulating the Sp1/NF-κB signaling pathway in esophageal squamous cell carcinoma. Int J Mol Sci. 2017;18(9):1833.

43. Dong G, Zhang S, Shen S, Sun L, Wang X, Wang H, et al. SPATS2, negatively regulated by miR-145-5p, promotes hepatocellular carcinoma progression through regulating cell cycle. Cell Death Dis. 2020;11(10):837.

44. Xu K, Li S, Yang Q, Zhou Z, Fu M, Yang X, et al. MicroRNA-145-5p targeting of TRIM2 mediates the apoptosis of retinal ganglion cells via the PI3K/AKT signaling pathway in glaucoma. J Gene Med. 2021;23(11):e3378.

45. Du Y, Zhang X, Zhang H, Chen Y, Zhu S, Shu J, et al. Propofol modulates the proliferation, invasion and migration of bladder cancer cells through the miR-145-5p/TOP2A axis. Mol Med Rep. 2021;23(6):439.

46. Wang S, Wang T, Gu P. microRNA-145-5p inhibits migration, invasion, and metastasis in hepatocellular carcinoma by inhibiting ARF6. Cancer Manag Res. 2021;13:3473–84.